Journal of Catalysis **201,** 258–269 (2001)
doi:10.1006/jcat.2001.3257, available online at http://www.idealibrary.com on IDEAL®

TPS, XPS, QEXAFS, and XANES Investigation of the Sulfidation of NiW/Al_2O_3–F Catalysts

Mingyong Sun,* Thomas Bürgi,* Riccardo Cattaneo,* Dick van Langeveld,† and Roel Prins*,[1]

*Laboratory for Technical Chemistry, Swiss Federal Institute of Technology (ETH), 8092 Zurich, Switzerland; and †Faculty of Applied Science, Delft University of Technology Julianalaan 136, 2628 BL Delft, The Netherlands

Received January 29, 2001; revised April 5, 2001; accepted April 19, 2001

The sulfidation behavior of alumina-supported Ni–W catalysts was investigated by means of temperature-programmed sulfidation (TPS), X-ray photoelectron spectroscopy (XPS), quick extended X-ray absorption fine structure (QEXAFS), and X-ray absorption near-edge structure spectroscopy (XANES). Either ammonium tetrathiotungstate or ammonium metatungstate was used as the precursor of tungsten, and nickel nitrate was the source of nickel. The effect of fluorination of the alumina support on the sulfidation behavior of tungsten and nickel on these two series of catalysts was studied as well. The sulfidation of the catalysts prepared from ammonium metatungstate passes through W(VI) oxysulfide intermediates. Fluorination of the alumina support aids the sulfidation of tungsten and nickel at low temperature and promotes the transformation of the W(VI) oxysulfide intermediates to WS_2. After sulfidation at 400°C and atmospheric pressure for 4 h, about 50% of tungsten and 60% of nickel in the catalysts prepared from ammonium metatungstate were sulfided. EXAFS showed that ammonium tetrathiotungstate supported on alumina decomposes to oxidic tungsten during the second impregnation with nickel nitrate. Nevertheless, sulfidation of the catalysts prepared from ammonium tetrathiotungstate is much easier. It also passes through W(VI) oxysulfide intermediates, and fluorination aids the formation WS_2. In the sulfided catalysts prepared from ammonium tetrathiotungstate and nickel nitrate, 100% of tungsten and nickel is in the sulfided state, but a small amount of tungsten is in a $\{WS_3\}$ state, with fully sulfided W(VI), rather than in the WS_2 state. The fluorine-containing catalyst contains a larger fraction of WS_2 than the fluorine-free catalyst.

Key Words: **TPS; XPS; QEXAFS; XANES; sulfidation; Ni; W; fluorination.**

1. INTRODUCTION

Alumina-supported nickel–tungsten catalysts are well known for their excellent hydrogenation activity (1–3) but poor sulfidability (4–6). The former property makes them attractive in the hydrotreating of heavy oil, in which catalysts with high activity for hydrodenitrogenation and hydrogenation of aromatics are required. The latter property indicates a direction for the development of better hydrotreating catalysts. To prepare better, fully sulfided Ni–W catalysts, it is essential to understand the mechanism of the sulfidation of alumina-supported Ni–W catalysts. A systematic temperature-programmed sulfidation (TPS) investigation of alumina-supported Ni–W catalysts revealed that sulfidation of Ni–W starts at room temperature and continues until 1000°C, and that calcination of catalysts at higher temperature makes the sulfidation more difficult (6). Temperature-programmed reduction of sulfidic alumina-supported Ni–W catalysts gave detailed information about the sulfidability of various species in alumina-supported nickel, tungsten, and Ni–W catalysts (7). Catalyst preparation parameters influence the sulfidation of the catalysts. Reinhoudt *et al.* established a relationship between the calcination temperature and the evolution of the active phase in alumina-supported Ni–W catalysts during sulfidation by applying high-resolution transmission electron microscopy (HRTEM), TPS (8), FTIR(NO), and XPS (9). Kishan *et al.* followed the state of nickel and tungsten during the TPS of Ni–W model catalysts on planar SiO_2 films on silicon substrates by X-ray photoelectron spectroscopy (XPS) and found that chelating agents could retard the sulfidation of nickel to a temperature where all tungsten had already been sulfided (10).

Two catalyst preparation methods have been shown to lead to catalysts with a higher degree of sulfidation. Incorporation of fluorine into an alumina support was found to favor the formation of larger WS_2 particles upon sulfidation (11, 12), and by using a thiosalt, instead of an oxysalt, fully sulfided tungsten catalysts could be obtained (12–14). Recently, we showed that catalysts prepared from the tetrathiotungstate thiosalt had a much higher activity in hydrodenitrogenation reactions than catalysts prepared from the metatungstate oxyanion (15). Combining TPS, XPS, and quick extended X-ray absorption fine structure measurements (QEXAFS), we studied the sulfidation behavior of W/Al_2O_3-F catalysts prepared from thiosalt and oxysalt (14). Because of the importance of alumina-supported

[1] To whom correspondence should be addressed. E-mail: prins@tech.chem.ethz.ch.

0021-9517/01 $35.00

Ni–W catalysts in industry, we extended our study of unpromoted tungsten catalysts to the corresponding nickel-promoted catalysts. The sulfidation behavior of nickel and tungsten in alumina-supported Ni–W catalysts prepared from thiosalt and oxysalt, as well as the effect of fluorine on the sulfidation of nickel and tungsten, was studied by means of TPS, XPS, QEXAFS, and X-ray absorption near-edge structure (XANES).

2. EXPERIMENTAL

Catalyst Preparation

Catalysts were prepared by means of the incipient wetness impregnation method. The preparation of the tungsten-only catalysts was described before (14). The fluorinated γ-Al_2O_3 support (denoted as Al_2O_3–F) was obtained by impregnation of the γ-Al_2O_3 with an aqueous solution of ammonium fluoride, followed by drying at 120°C for 4 h and calcination at 500°C for 4 h. The WO_3/Al_2O_3 and WO_3/Al_2O_3–F catalysts were obtained by impregnating the γ-Al_2O_3 and Al_2O_3–F with an aqueous solution of ammonium metatungstate followed by drying at 120°C for 4 h Calcination at 500°C for 4 h. The ATT/Al_2O_3 and ATT/Al_2O_3–F catalysts were obtained by impregnating the γ-Al_2O_3 and Al_2O_3–F supports with a solution of ammonium tetrathiotungstate ($(NH_4)_2WS_4$, ATT) in N,N-dimethylformamide to increase the solubility of ATT, followed by drying at room temperature in a vacuum desiccator. The nickel-promoted catalysts were prepared by impregnating the WO_3/Al_2O_3, WO_3/Al_2O_3–F, ATT/Al_2O_3, and ATT/Al_2O_3–F catalysts with a 0.3 M aqueous solution of $Ni(NO_3)_2 \cdot 6H_2O$ (Aldrich). After impregnation, the Ni–WO_3/Al_2O_3 and Ni–WO_3/Al_2O_3–F were dried at 120°C for 4 h and calcined at 500°C for 4 h. The Ni–ATT/Al_2O_3 and Ni–ATT/Al_2O_3–F were dried and kept in a vacuum desiccator at room temperature. The loading of tungsten and nickel was 10 and 1 wt%, respectively, in all catalysts, and the content of fluorine in the fluorinated catalysts was 1 wt%.

TPS Measurements

The procedure for the TPS measurements of nickel-promoted tungsten catalysts was the same as that for the unpromoted tungsten-only catalysts (14). The catalysts were sulfided in a quartz reactor with a mixture of H_2S, H_2, and Ar (3, 25, 72 vol%, respectively) at a total flow rate of 0.12 mol/h. After 0.5 h at room temperature, the samples were heated to 400°C (10°C/min) and kept at this temperature for 4 h. Thereafter, the temperature was increased to 1000°C (10°C/min), and kept at this temperature for 1 h to complete the sulfidation. The changes in the concentrations of H_2 and H_2S were recorded with a thermal conductivity detector and a UV detector, respectively.

XPS Measurements

Before the XPS measurements, 0.15 g of catalyst was first sulfided in a quartz reactor. After the sample was flushed with N_2 (99.999%) for 10 min at room temperature, the gas flow was switched to a 10 mol% H_2S/H_2 mixture (50 N cm^3/min), and the sample was heated from room temperature to 400°C at a rate of 5°C/min. The sample was kept in the H_2S/H_2 flow at 400°C for 4 h. Then the sample was cooled below 100°C and the gas flow switched to 50 N cm^3/min N_2 (99.999%). The sample was kept in the flow of N_2 until it cooled down to room temperature, then the inlet and the outlet of the reactor were closed. The reactor was opened in a glovebox ($O_2 < 10$ ppm) and samples were ground and pressed onto a stainless steel sample holder. A few drops of *n*-octane (Fluka, purity > 99.5, $H_2O < 0.02$%) were added on top of the sample. Then the sample holder was put into a plastic bottle and the bottle was closed in the glovebox. When the holder was mounted on the XPS machine the octane layer protected the sample from exposure to air.

XPS spectra were recorded on a Leybold Heraeus LHS11 apparatus (14). Spectra were recorded at a constant pass energy of 31.5 (W) and 63 eV (Ni). The Al(2*p*) line of Al_2O_3 at 74.7 eV (16) was used as internal standard to compensate for sample charging. The background was subtracted according to Shirley (17), and quantification was performed using the sensitivity factors reported by Wagner *et al.* (18). The weak W($5p_{3/2}$) line of W(IV) overlaps with the W($4f_{5/2}$) line of W(VI). This was accounted for by considering a W($5p_{3/2}$) line in the fit at 6 eV higher binding energy than the W($4f_{7/2}$) line with an intensity of 6% of the latter. The Ni($2p_{3/2}$) spectrum was used to quantify nickel in sulfidic and oxidic surrounding. Single mixed Gaussian–Lorentzian functions were used for nickel in sulfidic and oxidic environment and for the shake-up lines.

QEXAFS and XANES

The QEXAFS and XANES measurements were carried out at the X1 (RÖMO II) beam line of HASYLAB (Hamburg, Germany) (19, 20). The experimental procedure was the same as that for QEXAFS of the unpromoted tungsten catalysts (14). After collecting the spectra of the original samples in He atmosphere, the samples were sulfided *in situ* during data collection. A 60 ml/min stream of 10% H_2S in H_2 flowed through the cell while the sample was heated to 400°C at a rate of 3°C/min. The sample was then kept at 400°C for 30 min. Each scan took 6 min, which corresponded to a temperature interval of about 18°C during the temperature ramp. The XDAP program (version 2.2.2) was used to analyze and process the data (21). The pre-edge background was approximated by a modified Victoreen function, and the background was subtracted using a cubic spline routine. The spectra were normalized by

the edge jump. The k^3-weighted EXAFS functions were Fourier-transformed.

In the case of nickel, the spectra around the edge jump were fitted by a linear function of the measured oxidic and sulfided samples in order to estimate the fraction of sulfided nickel obtained at various sulfidation temperatures, using

$$\text{XANES observed} = f_1 \cdot (\text{XANES of oxidic state}) + f_2 \cdot (\text{XANES of sulfided state}),$$

where f_1 and f_2 are the fractions of the oxidic and sulfided states, respectively. Both f_1 and f_2 were treated as free parameters in this analysis. The reference for the oxidic state was the fresh Ni–WO_3/Al_2O_3 sample, whereas the reference for the sulfided state was the Ni–ATT/Al_2O_3–F sample sulfided at 400°C (30 min).

3. RESULTS

TPS Measurements

Figure 1 shows TPS patterns of the Ni–WO_3/Al_2O_3, Ni–WO_3/Al_2O_3–F, Ni–ATT/Al_2O_3, and Ni–ATT/Al_2O_3 –F catalysts. For each catalyst, the lower signal represents the change in the H_2 concentration of the effluent stream of the reactor and the upper signal the change in the H_2S signal. Negative peaks correspond to consumption and positive peaks to production of either H_2S or H_2. At the beginning of the temperature program, a small positive H_2S peak was recorded for the Ni–WO_3/Al_2O_3 and Ni–WO_3/Al_2O_3–F catalysts, which is due to desorption of adsorbed H_2S (6, 8, 14, 22). During the course of sulfidation, three H_2S consumption peaks (peaks S I, S II, and S III) and two H_2 consumption peaks (peaks H I and H II) were recorded. The three vertical lines in Fig. 1 indicate the maxima of the S I, S II, and S III peaks for the Ni–WO_3/Al_2O_3 catalyst. The amounts of the H_2S and H_2 that are consumed in the corresponding temperature ranges were calculated from the areas of the peaks. These results are given in Table 1. The standard deviations for the calculations of H_2S and H_2 consumption are ca. 10% (22). The amounts of the consumed H_2S and H_2 are normalized per mol of metal (nickel plus tungsten). The first H_2S consumption peak had no corresponding H_2 consumption, while the first H_2 consumption maximum corresponded to a minimum of H_2S consumption. Corresponding to the second H_2S consumption peak, a shoulder on the first H_2 consumption peak was recorded.

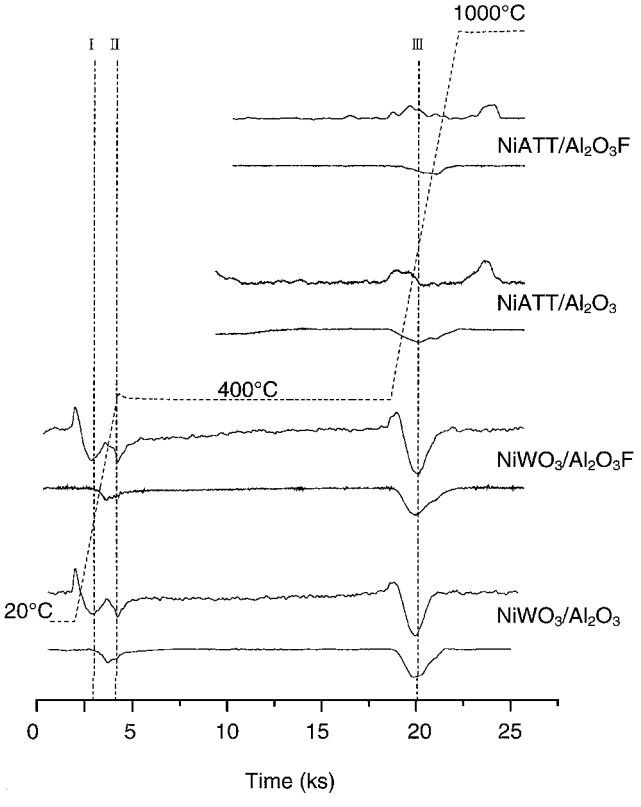

FIG. 1. TPS patterns of the Ni–WO_3/Al_2O_3, Ni–WO_3/Al_2O_3–F, Ni–ATT/Al_2O_3, and Ni–ATT/Al_2O_3–F catalysts with isothermal sulfidation at 400°C. The temperature program is indicated by the dashed line. Upper signal represents H_2S consumption (negative peak) and the lower signal the H_2 consumption.

TABLE 1

Consumption of H_2S and H_2 in TPS Measurements (mol/mol Ni + W)

	S I	S II	400°C H_2S	S III	H I	400°C H_2	H II
Ni–WO_3/Al_2O_3	0.23	0.16	0.58	0.71	0.17	0.21	0.46
Ni–WO_3/Al_2O_3–F	0.27	0.21	0.53	0.67	0.19	0.20	0.45
Ni–ATT/Al_2O_3				−0.30			0.29
Ni–ATT/Al_2O_3–F				−0.17			0.16

During the isothermal sulfidation at 400°C, the sulfidation of the catalysts proceeded so slowly that hardly any change in the H_2S and H_2 concentrations was recorded, and it was impossible to calculate directly how much H_2S and H_2 was consumed during this period. However, it is possible to estimate the amounts of H_2S and H_2 consumed during isothermal sulfidation from the amounts of H_2S and H_2 consumed during the other periods. Tungsten atoms are present on the support as WS_2 when they are fully sulfided (6–12, 14, 23). Even though the precise location of the nickel atoms at the WS_2 edge (24, 25) and their coordination by sulfur atoms in the sulfided (400°C) catalysts is still in debate, there is no doubt that nickel exists as Ni_3S_2 in a sulfidic atmosphere at high temperature (1000°C) (6, 7, 26). Sulfidation of one mole of nickel and tungsten (1 wt% nickel, 10 wt% tungsten) to Ni_3S_2–WS_2 will then consume 1.68 moles of H_2S and 0.84 mole of H_2. By subtracting the S I + S II + S III and H I + H II consumptions from these values, the amounts of H_2S and H_2 consumed during the 400°C isothermal sulfidation can be calculated. The accuracy for such an

estimation of H_2S and H_2 consumption should be in the same magnitude as those obtained during increasing temperature. The results are given in Table 1.

After 4 h isothermal sulfidation at 400°C, further increase of the temperature resulted in a continuous consumption of H_2 and H_2S until 850°C. Prior to the consumption of H_2S, the production of a small amount of H_2S was observed upon increasing the temperature. This part of H_2S was taken into account in the calculation of H_2S consumption between 400 and 850°C (S III).

Upon increasing the temperature at the beginning of the TPS measurements of the Ni–ATT/Al_2O_3 and Ni–ATT/Al_2O_3–F catalysts, a large amount of H_2S (out of recording range), accompanied by the consumption of a large amount of H_2, was formed due to the decomposition of ammonium tetrathiotungstate. Both the H_2S and the H_2 signal returned to the base line after 3 h of isothermal treatment at 400°C. When the temperature was further increased, a small amount of H_2S was produced, as in the case for the Ni-WO_3 catalysts. A broad H_2 consumption peak between 400 and 900°C was recorded for both Ni–ATT catalysts (H II, Table 2), but no corresponding H_2S consumption was observed. However, at 1000°C a H_2S production was recorded for both catalysts. The amounts of the produced H_2S were 0.30 and 0.17 mol per mole of nickel plus tungsten for the Ni–ATT/Al_2O_3 and Ni–ATT/Al_2O_3–F catalysts, respectively.

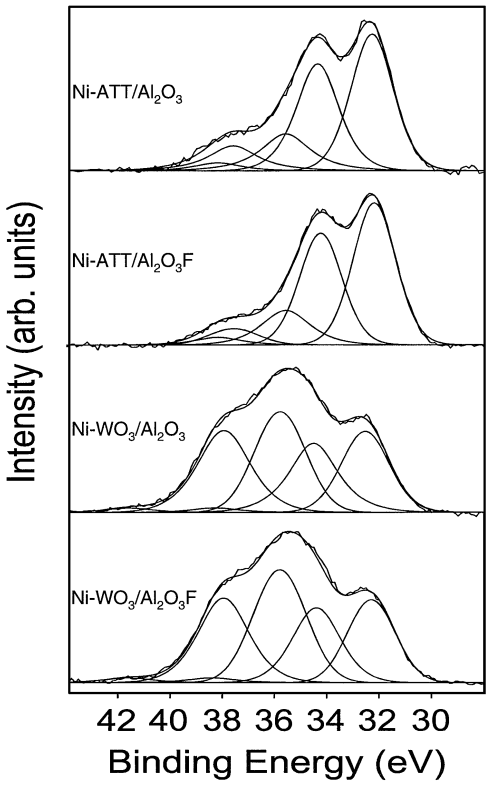

FIG. 2. W 4*f* XPS of the Ni–ATT/Al_2O_3, Ni–ATT/Al_2O_3–F, Ni–WO_3/Al_2O_3, and Ni–WO_3/Al_2O_3–F catalysts sulfided at 400°C and atmospheric pressure for 4 h with 10% H_2S in H_2.

XPS

Table 2 gives the fluorine, sulfur, tungsten, and nickel surface concentrations relative to aluminium of the investigated catalysts as determined by XPS. The theoretical values for the W/Al and Ni/Al ratios, in case tungsten and nickel are highly and homogeneously dispersed on the Al_2O_3 surface, are equal to 0.031 and 0.010, respectively. The Ni/Al ratios for all four catalysts were close to 0.010, while the W/Al ratios for the Ni–WO_3/Al_2O_3 and Ni–WO_3/Al_2O_3–F catalysts were also close to the theoretical W/Al value. For the Ni–ATT samples, the W/Al ratios were about 2/3 that of the Ni–WO_3 samples and of the theoretical value. The lower W/Al ratio in the Ni–ATT catalysts (Table 2) is due to the poorer dispersion of tungsten. The S/Al ratio was roughly the same for all samples. The S $2p_{3/2}$ binding energy was close to 162.2 eV for all samples, indicating sulfur with a formal charge of –2 (16). The F 1*s* binding energy in the fluorinated samples was 685.6 eV, typical for F^- on alumina (27).

TABLE 2

XPS Results of Sulfided Catalysts (400°C, 4 h)

	Ni–ATT/Al_2O_3	Ni–ATT/Al_2O_3–F	Ni–WO_3/Al_2O_3	Ni–WO_3/Al_2O_3–F
F/Al	—	0.096	—	0.078
S/Al	0.051	0.049	0.048	0.047
W/Al	0.017	0.020	0.029	0.030
Ni/Al	0.011	0.011	0.011	0.011
W_{sulf}/W_{to}	0.75	0.81	0.44	0.42
Ni_{sulf}/Ni_{to}	0.91	0.91	0.72	0.68
S/(Ni + W)	1.8	1.6	1.2	1.2

The W 4*f* XP spectra shown in Fig. 2 consist of two overlapping doublets arising from the $4f_{7/2}$ and $4f_{5/2}$ lines of W(IV) and W(VI). Deconvolution resulted in a $4f_{7/2}$ binding energy for W(IV) and W(VI) of 32.3 and 35.8 eV, characteristic of tungsten sulfide (WS_2) and tungsten oxide (WO_3), respectively (16). The individual peaks had a FWHM of 2.0 to 2.2 eV. The degree of sulfidation of tungsten ($W_{sulf}/W_{tot} = W(IV)/(W(IV) + W(VI))$, as determined from the fit and given in Table 2, was considerably higher for the Ni–ATT (75–81%) than for the Ni–WO_3 catalysts (42–44%). Fluorine only had a small effect on the degree of sulfidation.

The ratio of S/(W + Ni) for the fully sulfided catalyst is 1.76 if we assume that it only contains WS_2 and NiS after sulfidation at 400°C. Therefore, the extent of sulfidation of nickel and tungsten can also be estimated by the ratio of the measured value (Table 2) to the theoretical value of S/(W + Ni) ratio, being 1.0, 0.90, 0.68, and 0.65 for Ni–ATT/Al_2O_3, Ni–ATT/Al_2O_3–F, Ni–WO_3/Al_2O_3, and

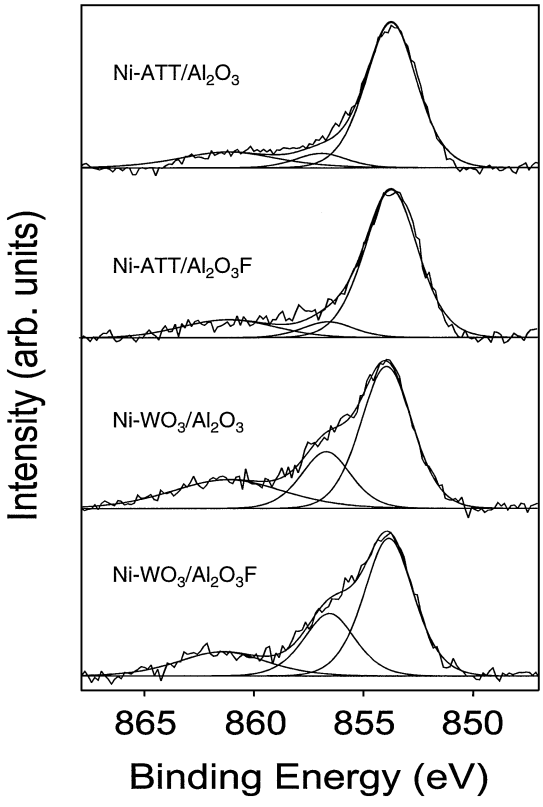

FIG. 3. Ni 2*p* XPS of the Ni–ATT/Al_2O_3, Ni–ATT/Al_2O_3–F, Ni–WO_3/Al_2O_3, and Ni–WO_3/Al_2O_3–F catalysts sulfided at 400°C and atmospheric pressure for 4 h with 10% H_2S in H_2.

Ni–WO_3/Al_2O_3F, respectively. This ratio has a similar trend as the ratio of W_{sulf}/W_{to}, indicating that the concentration of the sulfur on the surface is related the extents of sulfidation of tungsten and nickel.

Also, the Ni $2p_{3/2}$ spectra shown in Fig. 3 exhibited sizeable differences between the Ni–ATT and Ni–WO_3 samples. The deconvolution yielded peaks with FWHM of 2.8 to 2.9 eV at 853.8 and 856.6 eV. The binding energy of the first peak is indicative for nickel sulfide (4, 16, 27). The peak at 856.6 eV indicates Ni_2O_3 or $NiAl_2O_4$ but is not compatible with NiO, which exhibits a significantly lower Ni $2p_{3/2}$ binding energy (4). A characteristic feature of the Ni 2*p* spectrum is the shake-up satellite at 862–863 eV (Fig. 3), which has been assigned to a charge transfer transition (28). The intensity of the shake-up satellite depends on the coordination of nickel. The satellite is more intense for NiO than for Ni_2O_3 or $NiAl_2O_4$, which have nearly indistinguishable Ni $2p_{3/2}$ spectra (4). The relative intensities of the peak at 856.6 eV and the satellite (Fig. 3) are again compatible with Ni_2O_3 or $NiAl_2O_4$ but not with NiO.

The degree of sulfidation of nickel is expressed as the fraction of nickel sulfide out of total nickel (Ni_{sulf}/Ni_{to}) (Table 2). The nickel in the Ni–ATT samples was almost completely sulfided (91%), whereas for the nickel in the Ni–WO_3 catalysts the sulfidation degree was around 70%. Fluorine had no significant effect on the degree of sulfidation of nickel in the Ni–ATT catalysts, whereas a slightly lower sulfidation degree of nickel in the Ni–WO_3/Al_2O_3–F sample than in the Ni–WO_3/Al_2O_3 sample was observed.

QEXAFS

Figures 4 and 5 present the Fourier-transformed $\chi(k) \cdot k^3$ W L_{III}-edge QEXAFS spectra of the Ni–WO_3/Al_2O_3 and Ni–WO_3/Al_2O_3–F catalysts, respectively. In each case, the first spectrum was collected for the fresh sample, and the other spectra were obtained during sulfidation. The numbers next to the spectra denote the average temperatures during scans. The first spectrum has only one pronounced signal at 1.3 Å (not phase-corrected), due to a W–O contribution. This signal remains even after sulfidation at 400°C for 30 min (the last spectrum) for both Ni–WO_3/Al_2O_3 and Ni–WO_3/Al_2O_3–F catalysts. A signal at 2.0 Å (not phase-corrected) becomes significant upon sulfidation at 370 and 340°C for the Ni–WO_3/Al_2O_3 and Ni–WO_3/Al_2O_3–F catalysts, respectively. This peak is at the same distance as in WS_2 (23), and its appearance indicates the formation of WS_2. In addition to the W–O and the WS_2 signals, a signal is observed at 1.8 Å (not phase–corrected). It appears below 100°C and increases in intensity with sulfidation temperature until around 300°C and then decreases at higher sulfidation temperatures. This peak is at the same position as

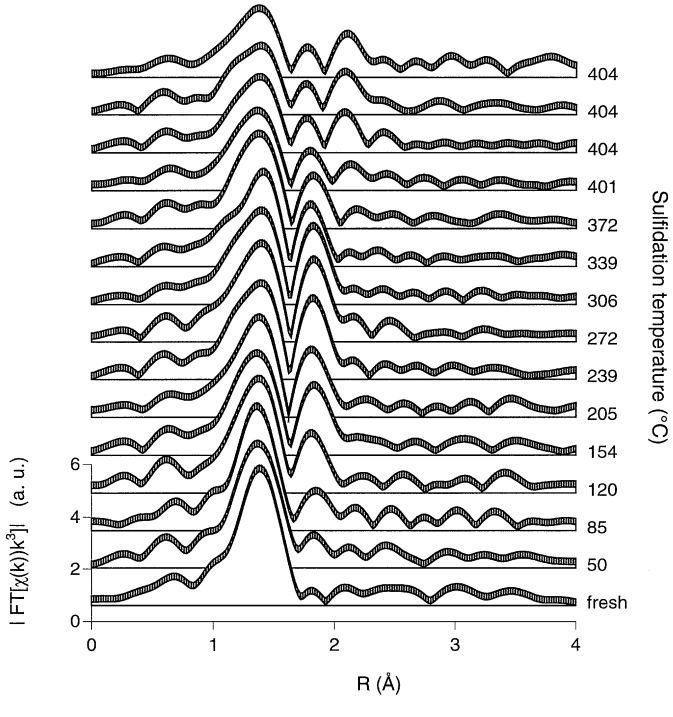

FIG. 4. Fourier transforms of the W L_{III} edge k^3-weighted QEXAFS functions measured during the sulfidation of the Ni–WO_3/Al_2O_3 catalyst.

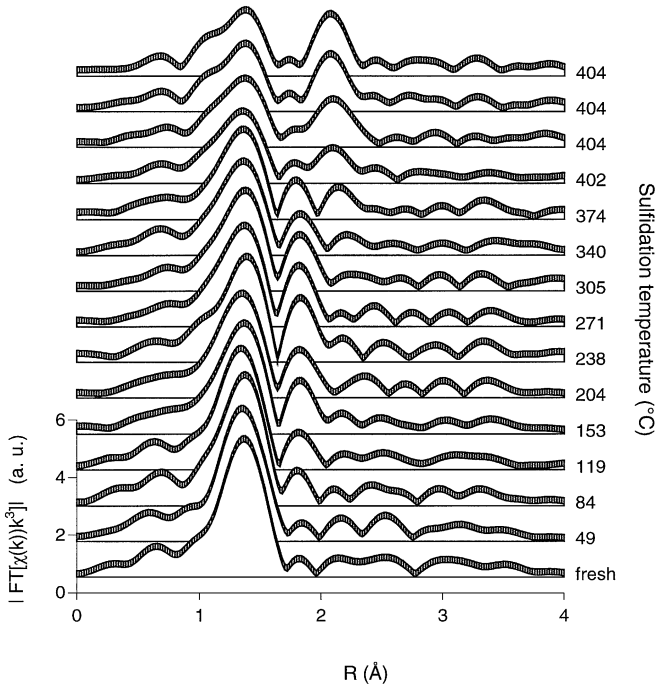

FIG. 5. Fourier transforms of the W L_{III} edge k^3-weighted QEXAFS functions measured during the sulfidation of the Ni–WO_3/Al_2O_3–F catalyst.

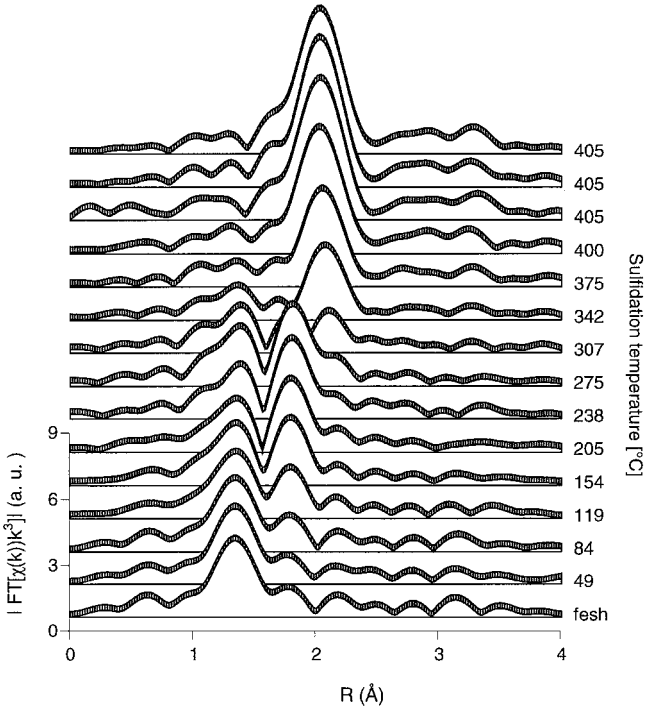

FIG. 6. Fourier transforms of the W L_{III} edge k^3-weighted QEXAFS functions measured during the sulfidation of the Ni–ATT/Al_2O_3 catalyst.

the peak observed in the spectrum of the fresh ATT/Al_2O_3 catalyst (14) and was attributed to sulfur atoms in the first coordination sphere of W(VI). This reveals that the sulfidation of tungsten in nickel-promoted tungsten catalysts to WS_2 passes through the same intermediates, containing W(VI) and sulfur, as in the unpromoted tungsten-only catalysts (14). For the Ni–WO_3/Al_2O_3–F catalyst, the intermediate signal (at 1.8 Å, not phase-corrected) is not as significant as in the spectra of the Ni–WO_3/Al_2O_3 catalyst and it is not detectable after sulfidation at 400°C. The intermediate still remains after sulfidation at 400°C for the Ni–WO_3/Al_2O_3 catalyst, however. After sulfidation at 400°C, the WS_2 signal for the Ni–WO_3/Al_2O_3–F catalyst is much stronger than that for the Ni–WO_3/Al_2O_3 catalyst, meaning that fluorine aids the transformation of the intermediate to the WS_2 phase.

Figures 6 and 7 show the Fourier–transformed $\chi(k) \cdot k^3$ W L_{III}-edge QEXAFS spectra of the Ni–ATT/Al_2O_3 and Ni–ATT/Al_2O_3–F catalysts, respectively. The first spectrum, which was collected for the fresh sample, shows that the tungsten atoms in the Ni–ATT catalysts are mainly coordinated by oxygen atoms (peak at 1.3 Å), and that only a small amount of sulfur atoms remained coordinated to tungsten (small peak at 1.8 Å), in contrast to the unpromoted ATT catalysts (14). This means that most of the sulfur atoms surrounding the tungsten atoms in the ATT catalysts were replaced by oxygen atoms during the impregnation of the ATT catalysts with the aqueous solution of nickel nitrate. Nevertheless, the resulting tungsten oxide species can be fully sulfided at 400°C. In addition to the signals at 1.3 and 1.8 Å, the QEXAFS spectra of the fresh Ni–ATT/Al_2O_3 and Ni–ATT/Al_2O_3–F samples also show a signal at about 3.1 Å, which was not observed

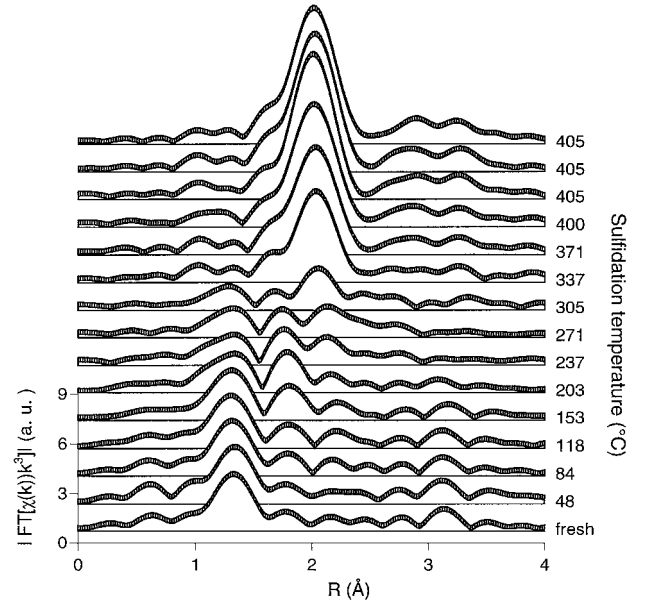

FIG. 7. Fourier transforms of the W L_{III} edge k^3-weighted QEXAFS functions measured during the sulfidation of the Ni–ATT/Al_2O_3–F catalyst.

for the Ni–WO_3 samples. This signal is attributed to a W–W coordination as in polytungstate. This polytungstate may be formed during the impregnation of ATT/Al_2O_3 with the nickel nitrate solution (see Discussion).

In the progress of transformation of the tungsten oxide species to the WS_2 phase, the 1.8 Å peak increased in intensity indicating that an intermediate was formed that has the same W–S distance as ATT and as the intermediate observed during the sulfidation of the Ni–WO_3 catalysts. The intermediate signal is stronger in the spectra for the Ni–ATT/Al_2O_3 catalyst than in the spectra for the Ni–ATT/Al_2O_3–F catalyst, and the WS_2 signal is stronger and became significant at a lower temperature for the Ni–ATT/Al_2O_3–F catalyst than for the Ni–ATT/Al_2O_3 catalyst. This result again indicates that fluorine favors the formation of the WS_2 phase. In the spectra of the sulfided Ni–ATT catalysts, W–W contributions (around 3.2 Å, not phase-corrected) are observed as well, which is not the case for the Ni–WO_3 catalysts, indicating that the WS_2 structure is better developed in the sulfided Ni–ATT catalysts.

There is no significant change in the Fourier-transformed $\chi(k)\cdot k^3$ Ni K-edge QEXAFS spectra collected during the sulfidation of the catalysts (not shown). It is difficult to distinguish the nickel sulfide and oxide environments. However, it is easy to distinguish the corresponding Ni K-edge XANES spectra (29). Figure 8 shows the Ni K-edge XANES spectra of the Ni–WO_3/Al_2O_3 and Ni–ATT/Al_2O_3 catalysts recorded before and after their sulfidation. All spectra of compounds with a not completely filled 3*d* band show a pre-edge feature due to a 1*s* to 3*d* transition. This feature varies with the number of *d* vacancies and symmetry

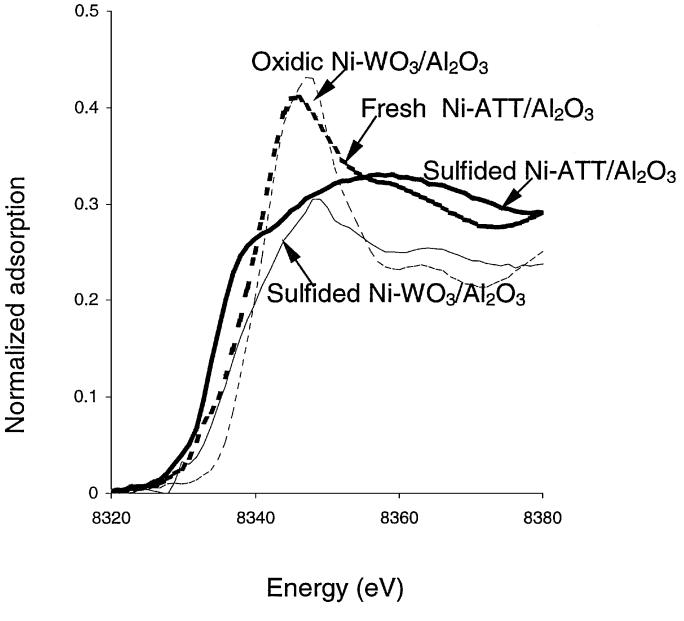

FIG. 8. XANES spectra at the Ni K edge for the Ni–WO_3/Al_2O_3 and Ni–ATT/Al_2O_3 catalysts before and after sulfidation.

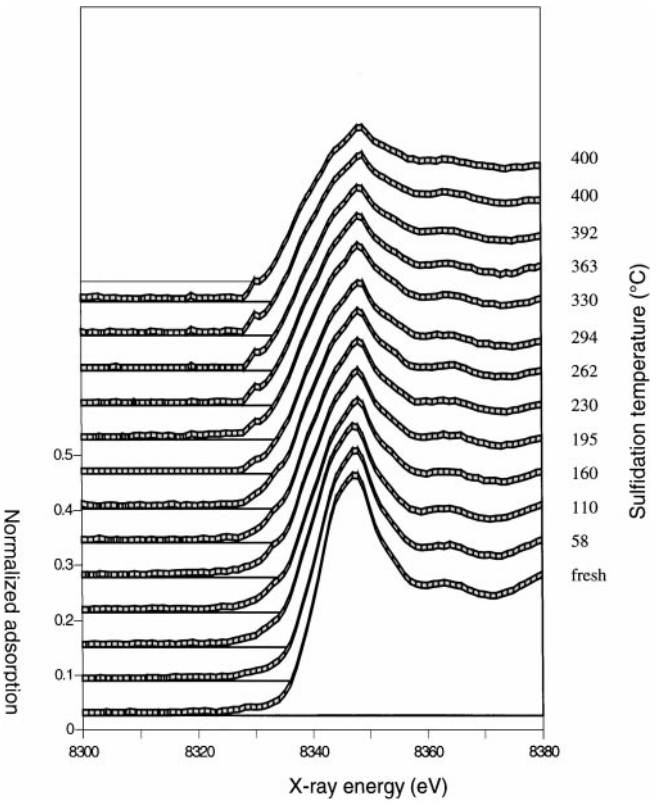

FIG. 9. XANES spectra at the Ni K edge measured during the sulfidation of the Ni–WO_3/Al_2O_3 catalyst.

of the absorbing atom site (30). The spectrum for the oxidic Ni–WO_3/Al_2O_3 catalyst shows the characteristic NiO pre-edge feature (29, 30). The large white line for the oxidic Ni–WO_3/Al_2O_3 catalyst at about 8347 eV is due to the presence of oxygen in the first coordination sphere of nickel. When all the oxygen atoms are replaced by sulfur atoms the white line disappears due to the nonionic character of the Ni–S bond (29, 31, 32). Therefore, the disappearance of the white line on the spectrum for the 400°C sulfided Ni–ATT/Al_2O_3 is a good indication of the complete replacement of oxygen atoms around nickel by sulfur atoms. The edge positions for the 400°C sulfided Ni–WO_3/Al_2O_3 and the fresh Ni–ATT/Al_2O_3 catalysts are between those of the oxidic Ni–WO_3/Al_2O_3 and the sulfided Ni–ATT/Al_2O_3 catalysts, which suggests the coexistence of oxidic and sulfidic nickel in the 400°C sulfided Ni–WO_3/Al_2O_3 and the fresh Ni–ATT/Al_2O_3 catalysts.

Figures 9 and 10 present a series of Ni K-edge XANES spectra measured during the sulfidation of the Ni–WO_3/Al_2O_3 and Ni–ATT/Al_2O_3 catalysts, respectively, to exhibit the progress of the sulfidation of nickel in these catalysts. The Ni K-edge XANES spectra for the Ni–WO_3/Al_2O_3–F and Ni–ATT/Al_2O_3–F (not shown) were similar to their fluorine-free counterparts. In order to quantify the sulfidation degree of nickel at various stages of

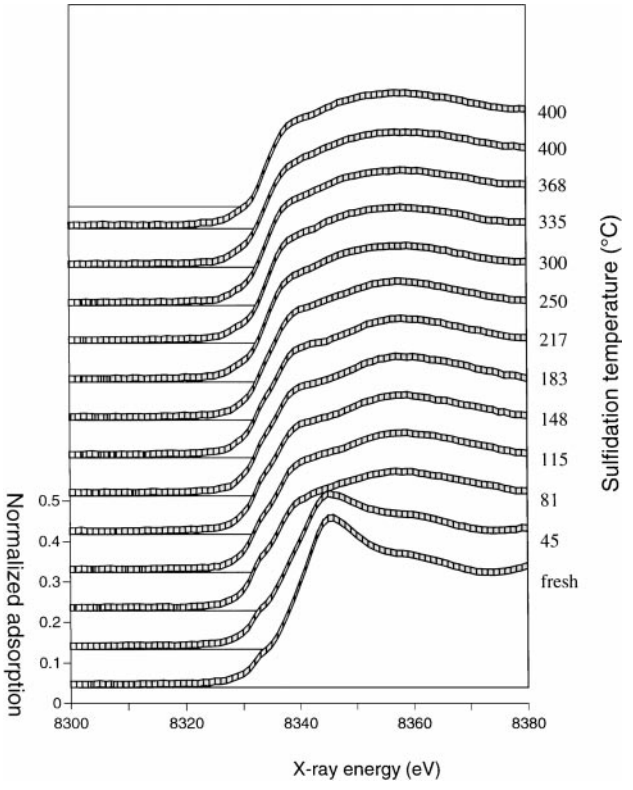

FIG. 10. XANES spectra at the Ni K edge measured during the sulfidation of the Ni–ATT/Al_2O_3 catalyst.

sulfidation, all XANES spectra were simulated by taking the oxidic Ni–WO_3/Al_2O_3 sample and the sulfided Ni–ATT/Al_2O_3–F sample (400°C, 30 min) as the references for the oxidic and sulfided states, respectively. The results (Fig. 11) show that 45 and 67% of the nickel in the fresh Ni–ATT/Al_2O_3 and Ni–ATT/Al_2O_3–F catalysts, respectively, had already been in the sulfided state, and that only about 60% of the nickel atoms in the Ni–WO_3/Al_2O_3 and Ni–WO_3/Al_2O_3–F catalysts were sulfided after sulfidation at 400°C. The sulfidation degree of nickel in the Ni–ATT catalysts after sulfidation at 100 to 200°C was even higher than 100%. It was also found that the fluorine-containing catalysts have a higher sulfidation degree than their fluorine-free counterparts when the sulfidation temperature is below 200°C.

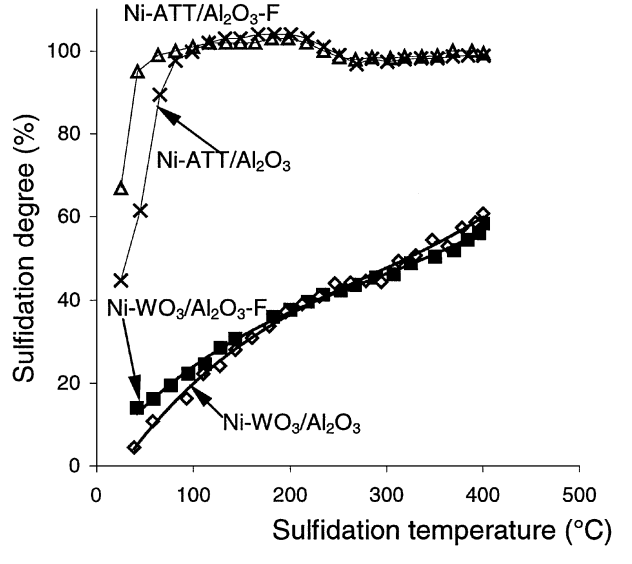

FIG. 11. Sulfidation profile of nickel in different catalysts, according to the XANES measurements.

4. DISCUSSION

The Catalysts Prepared from Oxysalt

The QEXAFS measurements show that part of the oxygen atoms surrounding the tungsten atoms in the Ni–WO_3 catalysts are already replaced by sulfur atoms below 100°C, and that the intermediate signal at 1.8 Å increases in intensity until 300°C (Figs. 4 and 5). The TPS results in Fig. 1 show that the first H_2S consumption peak at 200°C does not have a corresponding consumption peak of H_2. These results indicate that the replacement of oxygen by sulfur without reduction of tungsten is the dominant process below 300°C. Concerning the structure of the intermediates of sulfidation of tungsten, the QEXAFS measurements (Figs. 4 and 5) suggest that the intermediate, which appeared upon sulfidation below 100°C and decreased above 300°C, contains W=S contributions as in ATT. The present results do not allow to infer further details about the structure of the intermediate. A laser Raman spectroscopy study (33) showed that, after mild sulfidation at 227°C, the spectra of intermediates were similar to the spectrum of WS_3 and contained a band at 540 cm^{-1}, which was assigned to S_2^{2-} species.

At higher temperatures, the WS_2 signal increases at the expense of the signal of the intermediates (Figs. 4, 5). A shoulder on the first H_2 consumption peak is coupled with the second H_2S consumption peak at 400°C (Fig. 1). This means that the transformation of the $WO_{3-x}S_x$ intermediates to WS_2 becomes significant above 300°C. Sulfidation of WO_3/Al_2O_3 is a stepwise process (14); first, high oxidation state tungsten oxysulfides are formed, and then they are reduced to WS_2 at higher temperature. The stepwise sulfidation of tungsten in the catalysts can be expressed as

$$\{WO_3\} + xH_2S \rightarrow \{WO_{3-x}S_x\} + xH_2O \quad [1]$$

$$\{WO_{3-x}S_x\} + H_2 + (2-x)H_2S \rightarrow \{WS_2\} + (3-x)H_2O. \quad [2]$$

We write $\{WO_3\}$ to indicate that an oxidic W(VI) compound is sulfided, but that this compound does not necessarily consist of WO_3. It may as well consist of isolated tetrahedral tungstate oxyanions, as in $Al_2(WO_4)_3$. In the same way, we write $\{WO_{3-x}S_x\}$ to indicate that (most probably) a W(VI)

oxysulfide compound is formed by oxygen–sulfur exchange. The final $\{WS_3\}$ does not have to be the WS_3 structure (34), however. Analogously, $\{WS_2\}$ denotes a fully sulfided W(IV) compound which may have, but does not have to have, the WS_2 structure. Reaction [1] is dominant at low temperature (below 300°C), and at high temperature both reactions occur simultaneously.

Compared with the unpromoted WO_3/Al_2O_3 catalysts (14), the Ni–WO_3/Al_2O_3 catalysts consumed much more H_2S at low temperature (20 to 340°C, corresponding to the first H_2S consumption peak, see below). Simulation of the Ni K-edge XANES shows that about 49% of the nickel atoms in the Ni–WO_3 catalysts is sulfided at 340°C (Fig. 11). Thermodynamic data for nickel sulfides provided by Rosenqvist (26) indicate that NiS_{1+x} is the stable state in 10% H_2S/H_2 below 390°C. TPS of bulk NiO showed a $H_2S/Ni = 1$ consumption (no accompanying H_2 consumption) that corresponded to the formation of stoichiometric NiS at 180°C (6). The sulfidation of nickel oxide at low temperature can therefore be expressed as

$$\{NiO\} + H_2S \rightarrow \{NiS\} + H_2O. \qquad [3]$$

Like in the case for tungsten, {NiO} denotes nickel ions in an oxidic environment in the oxidic Ni–WO_3 catalysts and {NiS} denotes sulfided nickel that is formed during sulfidation at low temperature. They do not have to have the structure of NiO and NiS, respectively.

One mole of metal (nickel and tungsten) in our catalysts, with a loading of 1 wt% nickel and 10 wt% tungsten, contains 0.24 mol of nickel. Hence, sulfidation of 49% of nickel will consume 0.12 mol of H_2S. The remaining 0.11 mol of H_2S for the Ni–WO_3/Al_2O_3 catalyst, and 0.15 mol of H_2S for the Ni–WO_3/Al_2O_3–F catalyst (cf. S I in Table 1) must have been consumed by 0.76 mol of tungsten at low temperature. Fluorine aids the sulfidation of tungsten at low temperature. About half of the H_2S consumption in this temperature range is due to the sulfidation of nickel, even though nickel only makes up 24 mol% of the total amount of metal (nickel plus tungsten). This means that nickel is easier to sulfide than tungsten. Sulfidation of the WO_3/Al_2O_3 and WO_3/Al_2O_3–F catalysts consumed 0.10 and 0.12 mol H_2S per 0.76 mol of tungsten, respectively, in the same temperature range (14). The tungsten atoms in the nickel–tungsten catalysts consume slightly more H_2S in this temperature range than those in the tungsten-only catalysts, which means that nickel facilitates the sulfidation of tungsten.

Between the first two H_2S consumption peaks was a minimum in the H_2S consumption, which was accompanied by a consumption of H_2. The same phenomenon was also observed during the TPS of MoO_3/Al_2O_3 and ascribed to the hydrogenation of elemental sulfur (22). In a study of the basic steps in the sulfidation of crystalline MoO_3 to MoS_2, Weber *et al.* found that intermediate oxysulfides were formed between room temperature and 200°C, and that the oxysulfides were further converted to MoS_2 between 200 and 400°C (35). During this process S_2 ligands formed at low temperature were released at high temperature as H_2S. Therefore, the minimum of H_2S consumption in the TPS of MoO_3/Al_2O_3 is related to the transformation of intermediate oxysulfides to MoS_2. If a NiW/Al_2O_3 catalyst was not calcined at high temperature (only dried at 120°C), the minimum in H_2S consumption had a positive value, corresponding to the production of H_2S (8). The H_2 consumption at 340°C in the TPS of our Ni–W/Al_2O_3 catalysts corresponds to a H_2S production process. Nevertheless, the concentration of H_2S was still below the base line (Fig. 1), indicating that there still is a net H_2S consumption. It is clear that a H_2S production coincides with a simultaneous H_2S consumption in the TPS patterns of the Ni–WO_3/Al_2O_3 and Ni–WO_3/Al_2O_3–F catalysts. This H_2S production must be a nickel-related reduction process because the minimum in H_2S consumption did not have an accompanying H_2 consumption for the tungsten-only catalysts (6, 14). This H_2 consumption was ascribed to the reduction of $\{WS_3\}$ (8). The QEXAFS measurements (Figs. 4 and 5) and HREM measurements (8) show that WS_2 is formed at about 340°C during the sulfidation of Ni–WO_3/Al_2O_3 catalysts. Therefore, the H_2 consumption at 340°C during the TPS of the Ni–WO_3/Al_2O_3 catalysts is due to the transformation of $\{WS_3\}$ or $\{WO_{3-x}S_x\}$ intermediates to WS_2.

The maximum of the third H_2S consumption peak (S III, Table 1) for the Ni–WO_3 catalysts is at 640°C, which is much lower than that for the tungsten-only catalysts (750°C). This means that the nickel-incorporation also promotes the sulfidation of tungsten species that are more difficult to sulfide. The ratio of the H_2S to the H_2 consumed between 400 and 850°C (S III/H II, Table 1) is 1.5. If the sulfidation of Ni–WO_3/Al_2O_3 in this temperature range were a transformation of $\{WO_3\}$ and {NiO} directly to $\{WS_2\}$ and $\{Ni_3S_2\}$, the ratio of H_2S to H_2 should be 2. The fact that H_2S/H_2 ratio is below 2 indicates that $\{WS_3\}$ and {NiS}, formed at low temperature is reduced to $\{WS_2\}$ (Eq. [2]) and $\{Ni_3S_2\}$; (Eq. [4]) above 400°C:

$$3\{NiS\} + H_2 = \{Ni_3S_2\} + H_2S. \qquad [4]$$

Up to 400°C, the Ni–WO_3/Al_2O_3 catalyst consumed 0.97 mol H_2S and 0.38 mol H_2 per mole of nickel and tungsten (cf. Table 1). The XANES simulation shows that 60% of the nickel was sulfided after sulfidation of the Ni–WO_3/Al_2O_3 catalyst at 400°C (Fig. 11). Sulfidation of 60% of 0.24 mol of {NiO} to {NiS} consumes 0.14 mol H_2S and does not consume H_2. Hence, sulfidation of 0.76 mol tungsten in the Ni–WO_3/Al_2O_3 catalyst consumed 0.83 mol H_2S and 0.38 mol H_2. In the same way, sulfidation of 0.76 mol tungsten in the Ni–WO_3/Al_2O_3–F catalyst consumed 0.87 mol H_2S and 0.39 mol H_2.

TABLE 3

Tungsten Distribution of the Sulfided (400°C, 4 h) Catalysts in Percentage

	{WO_3}	{WS_3}	{WS_2}
Ni–WO_3/Al_2O_3	47	3	50
Ni–WO_3/Al_2O_3–F	45	4	51
Ni–ATT/Al_2O_3	0	28	72
Ni–ATT/Al_2O_3–F	0	11	89

According to reactions [1] and [2], sulfidation of α mole of {WO_3} to {WS_3} consumes 3 α mole of H_2S, and formation of β mole of {WS_2} consumes β mole of H_2 and produces β mole of H_2S. Thus, the total consumption of H_2S is 3α-β mole, and the total consumption of H_2 is β mole. For the Ni–WO_3/Al_2O_3 catalyst, sulfidation of 0.76 mol tungsten up to 400°C consumed 0.83 mol H_2S and 0.38 mol H_2, thus, $3\alpha - \beta = 0.83$, $\beta = 0.38$, and $\alpha = 0.40$. This means that after sulfidation of Ni–WO_3/Al_2O_3 at 400°C, the catalyst contained $100\,\beta/0.76 = 50\%$ {WS_2} and $100(\alpha - \beta)/0.76 = 3\%$ {WS_3}. In the same way, the sulfided Ni–WO_3/Al_2O_3–F catalyst contained 51% of {WS_2}, 4% of {WS_3}, and 45% of tungsten remained unsulfided. These results are listed in Table 3.

Table 2 gives the sulfidation degrees of nickel and tungsten (Ni_{sulf}/Ni_{to} and W_{sulf}/W_{to}, respectively) on the surface of the catalysts measured by XPS. According to the XPS results, fluorine slightly decreases the sulfidation of tungsten (from 44 to 42%) and nickel (from 72 to 68%) for the Ni–WO_3/Al_2O_3 catalyst. A similar result was reported by Benitez *et al.* (27). However, the TPS results show that fluorine slightly increases the degree of sulfidation, and the QEXAFS measurements (Figs. 4 and 5) show that the Ni–WO_3/Al_2O_3–F catalyst has a more pronounced WS_2 signal than the Ni–WO_3/Al_2O_3 catalyst after sulfidation at 400°C for 30 min. An analysis of surface population and architecture of the WS_2 crystallites of sulfided Ni–W/Al_2O_3–F catalysts made by Ramirez *et al.* with HRTEM showed that fluorine addition enhances the growth of the WS_2 structures significantly (12). XPS is a surface-sensitive technique and the signal from the deeper layers of the stacked WS_2 slabs will be attenuated. The slightly smaller fraction of W(IV) in the sulfided Ni–WO_3/Al_2O_3–F catalyst might thus be due to the lower dispersion of the WS_2 slabs.

The Ni K-edge XANES spectra of the 400°C sulfided Ni–WO_3/Al_2O_3 and Ni–WO_3/Al_2O_3–F catalysts are similar, meaning that fluorine does not influence the sulfidation degree of nickel to a significant extent. The quantitative simulation results show (Fig. 11) that the sulfidation of nickel proceeds faster at low temperature (below 200°C) and slower at high temperature in the fluorine-containing than in the fluorine-free catalyst, and that fluorine slightly decreases the sulfidation degree achieved at 400°C. Combining the TPS, XPS, QEXAFS, and XANES results, we conclude that fluorine favors the formation of the well-defined WS_2 structure and has no significant effect on the sulfidation degree.

The Catalysts Prepared from ATT

For the Ni–ATT catalysts, the consumption of H_2 between 400°C and 850°C was due to the reduction of {WS_3} to {WS_2} and {NiS} to {Ni_3S_2}. Nickel was fully sulfided (Fig. 11). Reduction of 0.24 mole of {NiS} to {Ni_3S_2} consumes 0.08 mol H_2. The remaining 0.21 and 0.08 mol H_2 (cf. Table 1) was consumed by reduction of {WS_3} to {WS_2} for the Ni–ATT/Al_2O_3 and Ni–ATT/Al_2O_3–F catalysts, respectively. According to reaction [2], one mole of {WS_3} consumes one mol of H_2. This means that the percentage of {WS_3} is 28% (0.21/0.76) in the 400°C sulfided Ni–ATT/Al_2O_3 catalyst, and 11% (0.08/0.76) in the 400°C sulfided Ni–ATT/Al_2O_3–F catalyst. The remaining tungsten exists as {WS_2}. These results are also given in Table 3. Reduction of the {NiS} and {WS_3} to {Ni_3S_2} and {WS_2}, respectively, will produce H_2S. The H_2S consumption was indeed observed but not parallel to the H_2 consumption. However, the amount of H_2S produced (0.30 and 0.17 mol per mole of nickel and tungsten for the Ni–ATT/Al_2O_3 and Ni–ATT/Al_2O_3–F catalysts, respectively) surprisingly matches the amount of H_2 consumed for the reduction of 0.24 mol of {NiS} to {Ni_3S_2} and 0.21 mol of {WS_3} to {WS_2} (cf. Table 3). Probably, the observed H_2S production was due to the reduction reactions, and the release of H_2S was delayed because of H_2S transport limitation.

Calcination aids the dispersion of the metal atoms on the alumina support. The Ni–WO_3 catalysts were calcined at 500°C for 4 h, while the Ni–ATT catalysts were not calcined at all. The much more pronounced W–W signal in the spectra of the sulfided Ni–ATT catalysts (Figs. 6 and 7) indicates that the WS_2 structures in the Ni–ATT catalysts are better developed than those in the Ni–WO_3 catalysts. The Ni K-edge XANES spectra of the Ni–ATT catalysts indicate that hardly any nickel is coordinated by oxygen after sulfidation at 400°C (Fig. 10). Nevertheless, the XPS results show that the percentage of sulfided nickel is 91% after 4 h sulfidation at 400°C. The remaining 9% of NiO on the surface of the Ni–ATT catalysts is probably due to the oxidation of nickel sulfide by trace amounts of oxygen during handling the samples in the glovebox. Because of the very low concentration of oxygen (10 ppm), the oxidation was probably limited to the surface nickel sulfide only. Because XPS is a surface-sensitive technique, XPS measured a lower degree of sulfidation than the bulk XANES technique.

Figure 11 shows that the sulfidation degree of nickel in the Ni–ATT catalysts seems to be higher than 100% upon sulfidation between 100 and 200°C, when the 400°C sulfided Ni–ATT/Al_2O_3–F catalyst is taken as the reference for a 100% sulfided sample. Probably, a slightly different nickel sulfide species, with higher XANES intensity than

the final state, was formed in this temperature range (100–200°C). Because it is also in the same temperature range that fluorine facilitates the sulfidation of nickel (Fig. 11), it is logical to propose that fluorine favors the formation of this nickel sulfide species. To confirm this, it is necessary to perform a series of classical nickel EXAFS measurements on the Ni–ATT catalysts after sulfidation at 150 and 400°C; this will be included in a future study.

Comparison of the QEXAF spectra of the fresh ATT/Al_2O_3 (Fig. 6 in Ref. 13) and Ni–ATT/Al_2O_3 (Fig. 6) catalysts shows that the impregnation of the ATT/Al_2O_3 catalyst with the aqueous solution of $Ni(NO_3)_2$ replaced most (but not all) of the sulfur atoms by oxygen atoms. Accompanying the loss of sulfur from tungsten, nickel was partially sulfided (Fig. 11). Nitrate anions, nickel cations, and water may have caused the change of ATT on the alumina support during the impregnation with the aqueous solution of $Ni(NO_3)_2$. Since also with nickel acetate (Fluka, >99.0%) part of the sulfur atoms around tungsten were replaced by oxygen atoms, nitrate is not the main cause for the decomposition of ATT. When ATT/Al_2O_3 particles were brought into water, the ATT slowly dissolved and the solution became yellow. The clear yellow solution was separated from the solid particles by filtration, and several drops of a nickel acetate solution (pH 8) were added to the yellow solution. Black solid particles precipitated, indicating that Ni(OH)S was formed. When a nickel nitrate solution (pH 4) was added to the yellow solution instead, no black particles formed, but the solution became brownish, probably due to the formation of $[Ni(WS_4)_2]^{2-}$ (36). Apparently, the pH value is an important factor to influence the reaction of ATT and nickel cations.

During the impregnation of the ATT/Al_2O_3 sample with the $Ni(NO_3)_2$ solution, part of the ATT dissolved. The WS_4^{2-} may react with Ni^{2+} to $[Ni(WS_4)_2]^{2-}$, which is not stable on the surface of alumina. Although the pH of the nickel nitrate solution is low, the pH on surface of the catalyst will increase during impregnation because of the buffer effect of alumina. Besides reacting with Ni^{2+}, ATT is also subject to partial hydrolysis in water to $WO_{4-x}S_x^{2-}$ and H_2S (37). Without Ni^{2+} this process is slow. Ni^{2+} reacts with H_2S to NiS, and thus accelerates the hydrolysis process. That is why the nickel on the fresh Ni–ATT/Al_2O_3 sample was partially sulfided and most of the sulfur atoms around tungsten were replaced by oxygen atoms. The Ni/W ratio is 0.3, thus, there is not enough nickel to complete the decomposition of the ATT compound. Indeed, the QEXAFS spectrum of fresh Ni–ATT/Al_2O_3 also showed that some sulfur atoms were still coordinated to tungsten (Fig. 6).

These newly formed WO_x species in the Ni–ATT catalysts are different from those in the impregnated and calcined Ni–WO_3/Al_2O_3 catalyst. The former WO_x species, which are the product of partial hydrolysis of WS_4^{2-} (37), are easier to sulfide than the latter (cf. Figs. 4 and 6). The Ni–WO_3 catalysts were calcined at 500°C, whereas the Ni–ATT catalysts were only dried at room temperature. High-temperature calcination aids the formation of W–O–Al linkages, which makes the sulfidation of tungsten more difficult (6). A Laser Raman study showed that the surface tungsten species in a WO_3/Al_2O_3 catalyst, which was calcined at 550°C, consisted of separate tetrahedrally coordinated WO_4^{2-} complexes when the loading of WO_3 was lower than 15% (38). In the QEXAFS spectra of fresh Ni–ATT/Al_2O_3 and Ni–ATT/Al_2O_3–F catalysts, a signal at 3.1 Å is clearly seen, which was not present in the spectra of the Ni–WO_3 catalysts. It is likely that the tungsten species in the fresh Ni–ATT catalyst form condensed structures. It is known that polyoxothiotungstates, such as $W_3OS_8^{2-}$ can be obtained from WS_4^{2-} in an organic solvent containing a little water (37). More work is needed to identify the structure of the condensed tungsten species in the Ni–ATT/Al_2O_3 catalyst.

Normally, sulfidation of the catalysts is performed at high pressure (e.g., 1.5 MPa) in industry. The properties of a final sulfided catalyst depend to a great extent on the sulfidation conditions (39–42). Higher temperature and partial pressure of H_2S accelerate sulfidation. The importance of the factors which affect the degree of sulfidation decreases in the following order: temperature > partial pressure of H_2S > duration of sulfidation. Conclusions drawn from the results obtained at atmospheric pressure are applicable to industrial operation.

5. CONCLUSIONS

The sulfidation of nickel–tungsten catalysts could be studied quantitatively by using a combination of techniques. XANES supplied the degree of sulfidation of nickel. The average degree of sulfidation of nickel and tungsten obtained from TPS then allowed to calculate the sulfidation degree of tungsten. By combining the H_2S and H_2 consumption during TPS, the amount of $\{WS_3\}$, formed as an intermediate in the sulfidation of tungsten, could be determined. Sulfidation of a classically prepared Ni–WO_3/Al_2O_3 catalyst at 400°C sulfides tungsten and nickel only partially. The tungsten species in the sulfided Ni–WO_3/Al_2O_3 catalyst are composed of 50% of $\{WS_2\}$, 3% of $\{WS_3\}$, and 47% $\{WO_3\}$, and in the sulfided Ni–WO_3/Al_2O_3–F catalyst of 51% of $\{WS_2\}$, 4% of $\{WS_3\}$, and 45% of $\{WO_3\}$ (measured by TPS). On the surface of the sulfided Ni–WO_3/Al_2O_3 catalyst, the fraction of sulfided nickel as measured by XPS is 72%, and that of W(IV) is 44%. Fluorination does not cause a significant change in the sulfidation degree, but it affects the sulfidation process and the composition of the final sulfided catalysts. Fluorination facilitates the sulfidation of nickel and tungsten at low temperature (below 200°C) and aids the transformation of tungsten oxysulfides to WS_2. The WS_2

structure is better developed in the sulfided Ni–WO_3/Al_2O_3–F catalyst than in the sulfided Ni–WO_3/Al_2O_3 catalyst.

Impregnation of alumina with ATT gives fully sulfided supported tungsten. During the subsequent impregnation with nickel nitrate, the tetrathiotungstate complex decomposes to tungsten oxide species. Sulfidation of the Ni–ATT catalysts at 400°C sulfides nickel completely and sulfides tungsten completely, but not completely to WS_2 (72% for Ni–ATT/Al_2O_3, and 89% for Ni–ATT/Al_2O_3–F). The WS_2 is better developed on the sulfided Ni–ATT catalysts than on the sulfided Ni–WO_3 catalysts. The tungsten oxide species formed in the fresh Ni–ATT catalysts are easier to sulfide than the tungsten oxide species in the classical Ni–WO_3 catalysts. This is of importance for the development of better sulfided tungsten catalyst in industry.

ACKNOWLEDGMENTS

B. M. Vogelaar and J. A. Moulijn (Delft University of Technology, The Netherlands) are gratefully acknowledged for their assistance with the TPS measurements and for fruitful discussions. The authors also thank the staff of the X1 station at HASYLAB and the colleagues who helped with the QEXAFS measurements. Discussions with Th. Weber and A. J. van der Vlies are also gratefully acknowledged.

REFERENCES

1. Ahuja, S. P., Derrien, M. L., and Le Page, J. F., *Ind. Eng. Chem. Prod. Res. Develop.* **9**, 272 (1970).
2. Stanislaus, A., and Cooper, B. H., *Catal. Rev. Sci. Eng.* **36**, 75 (1994).
3. Kabe, T., Qian, W., Funato, A., Okoshi, Y., and Ishihara, A., *Phys. Chem. Chem. Phys.* **1**, 921 (1999).
4. Ng, K. T., and Hercules, D. M., *J. Phys. Chem.* **80**, 2094 (1976).
5. Breysse, M., Cattenot, M., Decamp, T., Frety, R., Gachet, C., Lacroix, M., Leclerq, C., Mourques, L. de, Portefaix, J. L., Vrinat, M., Houari, M., Grimblot, J., Kasztelan, S., Bonnelle, J. P., Housni, S., Bachelier, J., and Duchet, J. C., *Catal. Today* **4**, 39 (1988).
6. Scheffer, B., Mangnus, P. J., and Moulijn, J. A., *J. Catal.* **121**, 18 (1990).
7. Mangnus, P. J., Bos, A., and Moulijn, J. A., *J. Catal.* **146**, 437 (1994).
8. Reinhoudt, H. R., van Langeveld, A. D., Kooyman, P. J., Stockmann, R. M., Prins, R., Zandbergen, H. W., and Moulijn, J. A., *J. Catal.* **179**, 443 (1998).
9. Reinhoudt, H. R., Crezee, E., van Langeveld, A. D., Kooyman, P. J., van Veen. J. A. R., and Moulijn, J. A., *J. Catal.* **196**, 315 (2000).
10. Kishan, G., Coulier, L., de Beer, V. H. J., van Veen, J. A. R., and Niemantsverdriet, J. W., *J. Catal.* **196**, 180 (2000).
11. Benitez, A., Ramirez, J., Vazquez, A., Acosta, D., and Lopez Agudo, A., *Appl. Catal.* **133**, 103 (1995).
12. Ramirez, J., Castillo, P., Benitez, A., Vazquez, A., Acosta, D., and Lopez Agudo, A., *J. Catal.* **158**, 181 (1996).
13. Ramanathan, K., and Weller, S. W., *J. Catal.* **95**, 249 (1985).
14. Sun, M., Burgi, Th., Cattaneo, R., and Prins, R., *J. Catal.* **197**, 172 (2001).
15. Sun, M., Bussell, M. E., and Prins, R., *Appl. Catal.*, in press.
16. Wagner, C. D., Riggs, W. M., Davis, L. E., Moulder, J. F., and Muilenberg, G. E., "Handbook of X-Ray Photoelectron Spectroscopy." Perkin–Elmer, Palo Alto, CA, 1979.
17. Shirley, D. A., *Phys. Rev. B* **5**, 4709 (1972).
18. Wagner, C. D., Davis, L. E., Zeller, M. V., Taylor, J. A., Raymond, R. M., and Gale, L. H., *Surf. Interface Anal.* **3**, 211 (1981).
19. Frahm, R., *Rev. Sci. Instrum.* **60**, 2515 (1989).
20. Tröger, L., *Synchr. Rad. News* **6**, 11 (1997).
21. Vaarkamp, M., Linders, J. C., and Koningsberger, D. C., *Physica B* **209**, 159 (1995).
22. Arnoldy, P., van den Heijkant, J. A. M., de Bok, G. D., and Moulijn, J. A., *J. Catal.* **92**, 35 (1985).
23. Louwers, S. P., and Prins, R., *J. Catal.* **139**, 525 (1993).
24. Byskov, L. S., Nørskov, J. K., Clausen, and Topsøe, H., *J. Catal.* **187**, 109 (1999).
25. Raybaud, P., Hafner, J., Kresse, G., Kasztelan, S., and Toulhoat, H., *J. Catal.* **190**, 128 (2000).
26. Rosenqvist, T., *J. Iron Steel Inst.* **176**, 37 (1954).
27. Benitez, A., Ramirez, J., Fierro, J. L. G., and Lopez Agudo, A., *Appl. Catal.* **144**, 343 (1996).
28. Kim, K. S., and Davis, R. E., *J. Electron Spectrosc.* **1**, 25 (1972).
29. Cattaneo, R., Shido, T., and Prins, R., *Stud. Surf. Sci. Catal.* **127**, 421 (1999).
30. Lytle, F. W., Greegor, R. B., and Panson, A. *J., Phys. Rev. B* **37**, 1550 (1988).
31. Lytle, F. W., Wei, P. S. P., Greegor, R. B., Via, G. H., and Sinfelt, J. H., *J. Chem. Phys.* **70**, 4849 (1979).
32. Louwers, S. P. A., Crajé, M. W. J., van der Kraan, A. M., Geantet, C., and Prins, R., *J. Catal.* **144**, 579 (1993).
33. Payen, E., Kasztelan, S., Grimblot, J., and Bonnelle, J. P., *Catal. Today* **4**, 57 (1988)
34. Hibble, S. J., Walton, R. I., Feaviour, M. R., and Smith, A. D., *J. Chem. Soc. Dalton* **16**, 2877 (1999).
35. Weber, Th., Muijsers, J. C., van Wolput, J. H. M. C., Verhagen, C. P. J., and Niemantsverdriet, J. W., *J. Phys. Chem.* **100**, 14,144 (1996).
36. Müller, A., and Diemann, E., *Chem. Commun.* **65** (1971).
37. Müller, A., Diemann, E., Jostes, R., and Bögge, H., *Angew. Chem. Int. Ed. Engl.* **20**, 934 (1981).
38. Salvati, L., Jr., Makovsky, L. E., Stencel, J. M., Brown, F. R., and Hercules, D. M., *J. Phys. Chem.* **85**, 3700 (1981).
39. Hallie, H., *Oil & Gas J.* Dec. 20, 69 (1982).
40. Yang, S. H., and Satterfield, C. N., *J Catal.* **81**, 168 (1983).
41. Prada Silvy, R., Grange, P., Delanny, F., and Delmon, B., *Appl. Catal.* **46**, 113 (1989).
42. van Gestel, J., Leglise, J., and Duchet, J. C., *J. Catal.* **145**, 429 (1994).